J. Microbiol. Biotechnol. (2010), **20**(3), 532–541
doi: 10.4014/jmb.0908.08038
First published online 20 January 2010

JOURNAL OF MICROBIOLOGY AND BIOTECHNOLOGY

Biochemical and Cellular Investigation of *Vitreoscilla* Hemoglobin (VHb) Variants Possessing Efficient Peroxidase Activity

Isarankura-Na-Ayudhya, Chartchalerm[1], Natta Tansila[1], Apilak Worachartcheewan[1], Leif Bülow[2], and Virapong Prachayasittikul[1]*

[1]*Department of Clinical Microbiology, Faculty of Medical Technology, Mahidol University, Bangkok 10700, Thailand*
[2]*Department of Pure and Applied Biochemistry, Center for Chemistry and Chemical Engineering, Lund University, Lund 22100, Sweden*

Received: August 30, 2009 / Revised: October 27, 2009 / Accepted: October 31, 2009

Peroxidase-like activity of *Vitreoscilla* hemoglobin (VHb) has been recently disclosed. To maximize such activity, two catalytically conserved residues (histidine and arginine) found in the distal pocket of peroxidases have successfully been introduced into that of the VHb. A 15-fold increase in catalytic constant (k_{cat}) was obtained in P54R variant, which was presumably attributable to the lower rigidity and higher hydrophilicity of the distal cavity arising from substitution of proline to arginine. None of the modifications altered the affinity towards either H_2O_2 or ABTS substrate. Spectroscopic studies revealed that VHb variants harboring the T29H mutation apparently demonstrated a spectral shift in both ferric and ferrous forms (406–408 to 411 nm, and 432 to 424–425 nm, respectively). All VHb proteins in the ferrous state had a λ_{soret} peak at ~419 nm following the carbon monoxide (CO) binding. Expression of the P54R mutant mediated the downregulation of iron superoxide dismutase (FeSOD) as identified by two-dimensional gel electrophoresis (2-DE) and peptide mass fingerprinting (PMF). According to the high peroxidase activity of P54R, it could effectively eliminate autoxidation-derived H_2O_2, which is a cause of heme degradation and iron release. This decreased the iron availability and consequently reduced the formation of the Fe^{2+}-ferric uptake regulator protein (Fe^{2+}-Fur), an inducer of FeSOD expression.

Keywords: *Vitreoscilla* hemoglobin, peroxidase-like activity, enzyme kinetics, catalytic constant, proteomic analysis, iron superoxide dismutase

Vitreoscilla hemoglobin (VHb) is a bacterial globin originated from the obligatory aerobic bacterium *Vitreoscilla* sp. The organism resides naturally in oxygen-limited environments such as stagnant ponds or decaying vegetative matters. The VHb has been thought to maintain an essential level of intracellular dissolved oxygen [44]. Nowadays, it has become a versatile tool in current biotechnology, especially for large-scale fermentation, since shortage of oxygen supply during cultivation can be overcome by heterologous expression of VHb. Cell growth and productivity are enhanced particularly under oxygen-depleted conditions [15, 23, 24]. Thus, VHb technology has been applied for industrial-scale production of many valuable compounds [45, 50].

Beside its role in O_2 delivery, VHb has been involved in various cellular activities, such as protein translation efficiency [3, 36], cellular metabolism [21], and alleviation of nitrosative stress [18, 22]. Recently, peroxidase-like activity has been disclosed in VHb [25, 38]. The steady-state kinetic study has revealed that VHb catalyzes the oxidation of various aromatic substrates *via* a ping-pong mechanism, as normally found in horseradish peroxidase (HRP) [25]. However, this catalytic activity seems to be limited possibly as a result of the improper nature of its active site. In comparison with HRP, two catalytically important residues (distal histidine and arginine) are missing in VHb, as illustrated in Fig. 1, which may account for the low activity. The distal histidine is believed to be a catalyst by firstly acting as a base to withdraw electron from H_2O_2 substrate and then turning to be an acid to donate hydrogen atom to heme-bound peroxide [28, 42]. This facilitates the cleavage of the peroxide bond yielding the release of a water molecule. Additionally, the positive charge of conserved arginine provides pulling force to this bond dissociation, which in turn accelerates compound I formation [35, 42].

In the present work, VHb variants possessing distal histidine and arginine residues have been constructed and determined the peroxidase kinetics in the assay reaction with H_2O_2 and aromatic substrate. Equivalent positions of

*Corresponding author
Phone: +662-441-4376; Fax: +662-441-4380;
E-mail: mtvpr@mahidol.ac.th

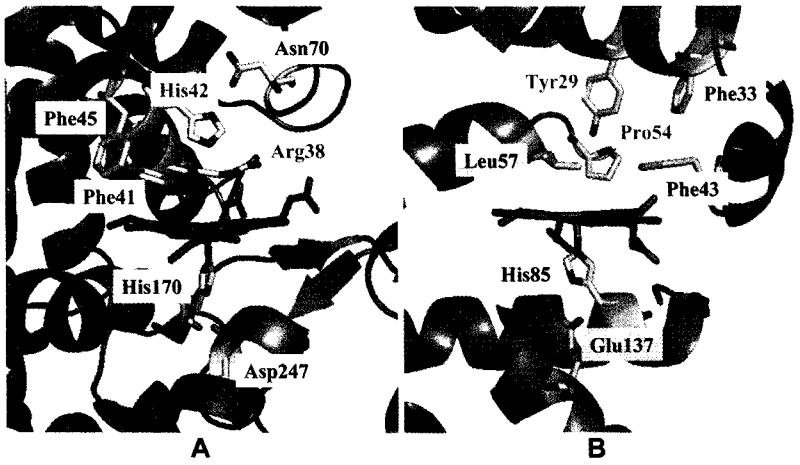

Fig. 1. Important residues in the heme cavity of HRP (**A**) and wild-type VHb (**B**).
The heme prosthetic group is shown in orange stick representation with oxygens and nitrogens in red and blue, respectively. In the distal site, conserved His42 and Arg38 of HRP are shown in grey stick representation (**A**) with blue label, and the equivalent positions are Tyr29 and Pro54 in VHb (**B**), respectively. Common residues (histidine and either aspartic or glutamic acid) in the proximal pocket of HRP and VHb are also shown. This figure was produced by molecular graphic software, PyMOL [12].

VHb, Tyr29 and Pro54, as found in HRP, have been selected for mutagenic modifications. Proteomic study has also been exploited to observe the consequence of VHb expression on protein profiling of *E. coli*. Such finding would suggest an additional role of this oxygen-binding protein when it behaves as a H_2O_2 detoxifying enzyme.

MATERIALS AND METHODS

Bacterial Strain and Chemical Reagents

Cloning and expression of each VHb variant were conducted in *Escherichia coli* strain TG1 (lac-pro), *Sup* E, *thi* l, *hsd* D5/F' *tra* D36, pro A^+ B^+, *lac*I, *lac*Z, M15 (*ung*$^+$, *dut*$^+$). PCR-based site-directed mutagenesis of the VHb gene was carried out using pV6h as a template [25]. Mutagenic primers were purchased from MWG Biotech (Ebersberg, Germany). 2,2'-Azino-bis (3-ethylbenzothiazoline-6-sulfonic acid) (ABTS) and hydrogen peroxide [30% (v/v) H_2O_2, $\varepsilon_{230\,nm}$=72.8 M^{-1} cm^{-1}] [20] were obtained from Sigma and Aldrich, respectively. Before use, the H_2O_2 solution was standardized and freshly prepared using the corresponding molar adsorption coefficient described above. Other reagents were of analytical grade and commercially available.

Site-Directed Amino Acid Substitution of Distal Residues of VHb

Selected residues (Tyr29 and Pro54) in the distal pocket of VHb were substituted with histidine and arginine, respectively, in order to simulate the active site of typical peroxidase. The *vhb* gene was amplified by using single-mutation-containing primers as follows: (Y29H_F: 5'-ATTACCACGACTTTT**CAT**AAAAACTTGTTTGCC-3'; P54R_F: 5'-GAATCTTTGGAGCAG**CGT**AAGGCTTTGGCGATG-3', mutations shown in bold). Complete digestion of parental plasmid DNA was enabled by addition of *Dpn*I restriction enzyme to the PCR product (37°C for an hour). DNA with desired mutation was then transformed into *E. coli* TG1 competent cells and cultured overnight at 37°C on Luria–Bertani (LB) agar supplemented with 100 μg/ml ampicillin (Amp). Colonies were selected randomly for plasmid isolation. Verification of the correct mutation on each plasmid was carried out by DNA sequencing (BM Labbet, Lund, Sweden). A double mutant, Y29H/P54R, was generated by introducing the P54R mutation into the pV6H_Y29H mutant plasmid.

Expression and Purification of VHb Mutants

E. coli TG1 cells carrying plasmids coding for native VHb and its variants (Y29H, P54R, and Y29H/P54R) were cultivated in modified LB medium (10 g tryptone, 10 g yeast extract, and 5 g NaCl, pH 7.2–7.4) supplemented with 100 μg/ml ampicillin and 0.3 μM δ-aminolevulinic acid (δ-ALA; heme precursor) [7], at 37°C, 150 rpm. Once cell density (OD_{600}) reached 0.6–0.8, recombinant VHb proteins were actively produced as a consequence of gene induction by isopropyl-β-D-1-thiogalactopyranoside (IPTG) at 0.5 mM final concentration. Then, cultures were further incubated at 30°C, 150 rpm for 14–16 h. Reddish cells indicating the hemoglobin expression were collected, washed, and ruptured by ultrasonic disintegration. Crude cell extracts were centrifuged at 13,000 ×g, 4°C for 15 min and the supernatant was collected. Before loading onto an affinity column, the supernatant was dissolved in lysis buffer (100 mM Tris-HCl containing 0.5% Triton X-100, pH 8.0) and filtered through a 0.2-μm polycarbonate membrane. The presence of a polyhistidine tag allowed VHb proteins to be purified *via* Ni^{2+}-IDA chromatography. Bound proteins were released from the gel matrix upon applying a gradient of imidazole solution (up to 0.5 M). Reddish fractions were pooled and subsequently dialyzed against 100 mM Tris-HCl, pH 8.0, to remove imidazole. Protein was quantified by the Bradford dye-binding assay [11] with bovine serum albumin (BSA) as a standard and its homogeneity was determined by sodium dodecyl sulfate–polyacrylamide gel electrophoresis (SDS–PAGE). Purified protein (>95% purity) was utilized in all experiments.

Spectroscopic Measurements of VHb Proteins

UV–Vis spectra of VHb variants (5 μM in 50 mM sodium phosphate buffer, pH 7.5) were recorded at room temperature on a DU 800

UV/Vis spectrophotometer (Beckman Coulter, U.S.A.). In addition, changes in the Soret peak were monitored following chemical reduction or oxidation (by excess amount of sodium dithionite or ammonium persulfate, respectively) as well as CO-binding in the same buffer.

Measurement of Peroxidase Kinetics of VHb Variants

The oxidations of reducing substrate, ABTS, by mutant proteins were determined using the DU 800 UV/Vis spectrophotometer. Initial rates for the one-electron oxidation of ABTS substrate in the presence of H_2O_2 were measured over the first 30 s at ambient temperature. It is worth to note that concentrations of H_2O_2 and reducing substrate were in enormous excess compared with VHb concentration to ensure the pseudo-first-order reaction. A 1-ml reaction mixture in 50 mM sodium phosphate buffer, pH 7.5 containing 0.5 μM VHb proteins, 3–75 mM H_2O_2, and 100–500 μM ABTS was used. Triplicate measurements were performed for each point of substrate concentration. The initial velocity for the formation of $ABTS^{+}$ radical was obtained by Beer's law using its extinction coefficient of $\varepsilon_{660\,nm}$=14.7 mM^{-1} cm^{-1} [1]. Consequently, it was used for plotting and calculation of kinetic parameters including k_{cat} and K_m for both H_2O_2 and ABTS substrates.

Moreover, the rate of compound I formation (k_1) was measured at ambient temperature [26] in 50 mM sodium phosphate, pH 7.5. The concentration of H_2O_2 substrate was varied over the range of 3–75 mM at 200 μM ABTS reducing substrate and 0.5 μM VHb protein. Rate constants were obtained by fitting the recorded data to pseudo-first-order reaction using the epsilon value of the $ABTS^{+}$ radical described above.

Preparation of Protein Samples for Proteomic Experiment

E. coli TG1 expressing wild-type VHb or its variants was grown aerobically at 37°C, 150 rpm in 5 ml of LB medium supplemented with 100 μg/ml ampicillin, and then a 100 dilution of the pre-culture was made into 50 ml of LB/Amp broth. This culture was incubated further for 16 h at the same condition. To induce VHb expression, 1 mM IPTG was added into the bacterial culture during the exponential phase (OD_{600} 0.6–0.8). After collecting cells by centrifugation (4,500 ×*g*, room temperature, 10 min), cells were washed three times using 40 mM Tris-HCl, pH 8.0, to remove residual salts and other chemicals. Cells were then dissolved in 1 ml Tris-HCl buffer, pH 8.0. Lysis buffer (250 μl), freshly prepared before use by mixing 10 mg/ml dithiothreitol (DTT) and 10 μg/ml protease inhibitor cocktail into 7 M urea, 2 M thiourea, and 4% CHAPS, was added into the cell suspension. A clear supernatant containing total proteins was then obtained by ultrasonic disintegration (Branson Sonifier Model 450) followed by centrifugation at 13,000 ×*g* for 30–60 min at room temperature. Bradford's method was used for determination of protein concentration using BSA as a standard. Subsequently, the cellular extract was mixed with 1 M acrylamide (1:10 of total volume), left at room temperature for 10 min, and then stored at −20°C until use.

Two-Dimensional Gel Electrophoresis (2-DE)

Experiments were performed according to procedures described previously [21]. Briefly, protein sample was examined using a 2D electrophoresis set purchased from Atto Corporation, Japan (IEF disc gel and mPAGE; Models AE-6541 and AE-6531). All procedures were done in accordance with the manufacturer's recommendation with minor modifications. One hundred μg of cellular proteins was carefully loaded on the top of pre-casting IEF rod gels with pH range of 3–10 (Atto Corporation). The gel was overlaid with 150 μl of upper electrode buffer (0.2 M NaOH). This first-dimension electrophoresis was operated at 300 volts for 3.5 h. Diffusion of proteins from the agarose gel was prohibited by soaking the 1D gel in 2.5 g% trichloroacetic acid (TCA) for 3 min. Fixed gels were then washed 3 times with distilled water. Before performing the second-dimension electrophoresis, gels were immersed in SDS equilibration buffer [50 mM Tris-HCl, 6 M urea, 30% (v/v) glycerol, 2% SDS and bromphenol blue, pH 8.8] for 10 min. After that, rod gels or Whatman filter paper dotted with standard protein markers were placed onto the pre-casting gradient (5–20% acrylamide) SDS–PAGE gel (Atto Corporation). All components were connected to one another by sealing with 1% agarose gel. Second-dimension gels were electrophoresed initially at 10 mA for 10 min and subsequently run at 40 mA for 90 min. Colloidal Coomassie blue was used to stain gels with mild agitation (20–25 rpm) for 2–3 h. Gels were then washed several times with distilled water to remove unstained dye and finally photographed.

Protein Identification by Peptide Mass Fingerprinting (PMF)

Protein spots on gels were taken out manually and placed into 96-well plates filled with 50% methanol and 5% acetic acid. Each of the protein spots was digested by high-grade trypsin (Promega, U.K.), mixed with spotter solution (10 mg/ml α-cyano-4-hydroxycinnamic acid dissolved in 66% acetonitrile and 0.1% trifluoroacetic acid), and then spotted onto a 384-well target plate (Bruker Daltonics, Germany). Protein digestion and spotting were carried out using a Spot Handling Workstation (GE Heathcare, U.S.A.). Digested proteins were shot with approximately 500 laser beams for acquisition of mass spectra, which were then matched in the NCBInr database using BioTool 2.0 (Bruker Daltonics) and MASCOT 2.2 software (MatrixScience, http://www.matrixscience.com). Permission of only 1 incorrect cleavage per peptide and a score of ±1 kDa initial mass tolerance were applied in all searches. Protein identification was confidently decided if the score of matched proteins was greater than 80 (p<0.05).

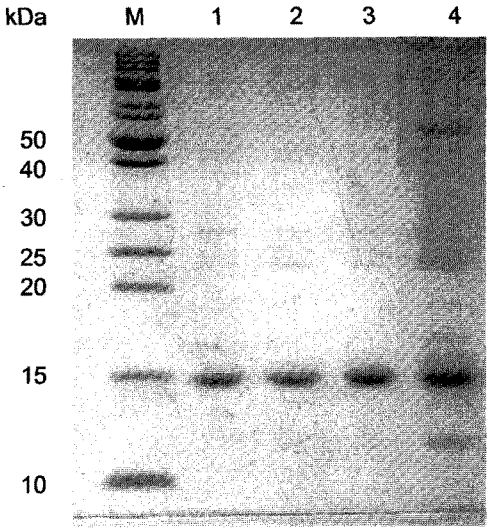

Fig. 2. SDS–PAGE showing purified proteins of all VHb variants: molecular mass marker (M); wild-type VHb (1); and Y29H (2); P54R (3); and Y29H/P54R (4) variants.

RESULTS

Construction of VHb Variants and Investigation of Their Spectral Properties

Three VHb variants (designated as Y29H, P54R, and Y29H/P54R) were successfully constructed in which the target residues were initially identified with the aid of molecular modeling served by PyMOL [12]. Supplementation of δ-ALA, a heme precursor, to cultures significantly improved heme content, which could be readily observed by the increase of pellet reddishness [7] (data not shown). After purification by Ni^{2+}-IDA affinity chromatography, the wild-type VHb and its variants showed approximately >95% homogeneity as located at ~16 kDa (Fig. 2). To investigate the spectral properties of VHb proteins in ferric, ferrous, and carbonyl forms, ammonium persulfate and sodium dithionite were added in excess to the hemoglobin solution prior to acquiring the spectra. For CO-bound form, VHb protein was treated with dithionite followed by exposure to CO gas for a few seconds. Fig. 3 shows that the UV–Vis spectra of wild-type VHb and P54R variants were nearly identical, and their untreated proteins were likely to be in a ferric state, with Soret peaks positioned at 406 and 408 nm, respectively. Y29H and Y29H/P54R variants revealed unusual absorption properties in which the Soret maxima were shifted to 411 nm. These positions were usually close to the oxy-form (λ_{Soret}=414 nm) but they lacked typical peaks at 543 and 576 nm known as α-bands [27]. Instead, they showed a broad minor peak at 534 nm. To verify whether they were in oxygenated form, both protein samples were bubbled with CO gas and the spectra were then recorded. However, interconversion of oxygenated protein, if formed, to CO-bound protein was not detected (data not shown) since exposure to CO gas of oxygenated VHb has been proven to change the absorption peak to 419 nm [27]. Therefore, these findings indicated that all protein samples were present in the ferric form. Other confirmative evidences revealed that further addition of ammonium persulfate did

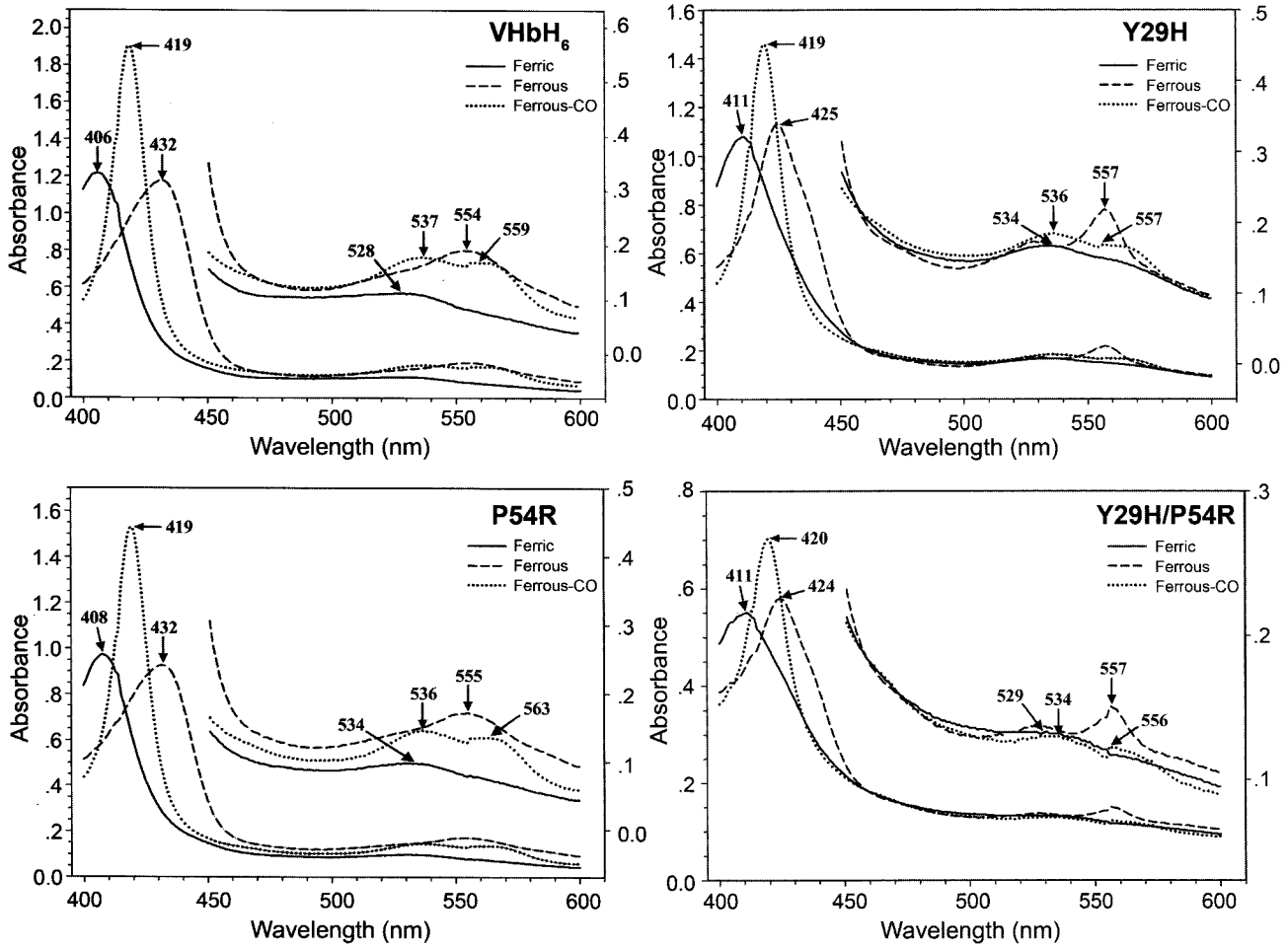

Fig. 3. UV–Vis spectra of VHb samples (5 μM) in 50 mM sodium phosphate buffer, pH 7.5. Ferrous or reduced form (dashed line) was obtained following the addition of excess dithionite into ferric-VHb (solid line); and CO complex (dotted line) was obtained by exposing the ferrous-VHb to CO gas for a few seconds. The absorption spectra in the visible region starting at 450 nm were magnified, and the scale is indicated on the right.

Table 1. The steady-state kinetic properties of VHb variants in reaction with aromatic substrate ABTS in the presence of H_2O_2.

VHb proteins	k_{cat} (s^{-1})	K_m (H_2O_2) (mM)	K_m (ABTS) (μM)	k_1 (M^{-1} s^{-1})
$VHbH_6$	0.81±0.03	11.72±1.23	55.38±10.11	30.73±0.69
Y29H	0.20±0.03	30.83±5.14	160.54±47.25	4.89±0.63
P54R	11.80±2.79	22.26±1.33	3,238.79±623.07	23.08±0.24
Y29H/P54R	0.18±0.06	9.13±0.87	1,686.81±699.13	1.17±0.14

Measurements were performed in 50 mM sodium phosphate buffer, pH 7.5, at room temperature.

not alter the spectra (data not shown). Meanwhile, treatment of VHb proteins with excess dithionite produced a 432-nm peak for the wild type and the P54R variant, and a 425-nm peak for Y29H and Y29H/P54R variants. As expected, CO complexes of all proteins appeared at 419 nm. However, slightly different peaks in α-bands among each protein were observed, as shown in Fig. 3, in which two minor peaks were found at 534–537 and 556–563 nm.

Steady-State Kinetics of VHb Variants

Initial rates of formation of $ABTS^+$ radical upon reacting with H_2O_2 were determined and calculated by Beer's law as mentioned earlier. Results of the enzymatic characterization are summarized in Table 1. Expectedly, the P54R variant possessed approximately 15-fold increase in catalytic constant (k_{cat}) for the peroxidase-catalyzed reaction compared with that of the wild-type VHb (11.80 and 0.81 s^{-1}, respectively). More importantly, such catalytic constant was approximately 60-fold higher than those of the Y29H and Y29H/P54R variants (0.20 and 0.18, s^{-1}, respectively). However, a 2-fold lower K_m for H_2O_2 was observed, suggesting that the substituted positively charged amino acid could not potentially afford binding to the H_2O_2 substrate. The rate of compound I formation (k_1) also revealed that this substitution slightly decreased the reactivity towards the H_2O_2 molecule. As evidenced in the other two variants, the Y29H mutation reduced the catalytic constant by a factor of 4 as well as the K_m for H_2O_2 and ABTS substrates by a factor of 1–3 and 3–30, respectively. Likewise, k_1 constants for compound I formation of variants Y29H and Y29H/P54R were decreased by factors of ~6 and 26, respectively, compared with the wild-type VHb. Thus, the Y29H mutation seemed to considerably abolish the formation of compound I intermediate. This finding correlated well with the lower affinity to H_2O_2 substrate as mentioned previously.

Effects of VHb Variants on Protein Expression Profiles of *E. coli*

To further investigate whether the high efficiency to catalyze the peroxidase reaction of the VHb variants rendered any alterations or consequent effects on the cellular responses of host cells, total protein extract was analyzed by a proteomic approach. After 2-DE experiment, two areas of each gel displaying protein spots with either down- or upregulation were zoomed, and those of the wild type VHb are displayed in Fig. 4A. Several protein spots (Fig. 4B) were selected and identified by mass spectrometry and the results are summarized in Table 2. As shown in Fig. 4C, molecular chaperones DnaK and GroEL were highly expressed and are usually stated as landmarks in several proteomic analyses (nos. 1, 2, 12, 17, 24, and 3, respectively). The levels of alkyl hydroperoxide reductase (AhpC), thiol peroxidase (Tpx), rotamase B, and DNA protection protein (Dps) remained unchanged. The monomeric subunit of bacterial hemoglobin (represented as spots no. 9, 10, 11, 16, 21, 22, and 25) could readily be visualized at molecular mass of ~16 kDa and *p*I value of ~5.3. However, notification has to be made that expression levels of each VHb variants were not equal. Single amino acid substitution adversely affected the expression level of VHb proteins as determined by the intensity of protein bands ($VHbH_6$>P54R>Y29H>Y29H/P54R). Obviously, the double mutant (Y29H/P54R) was poorly expressed in comparison with others. This suggests that the position of the amino acid residue in the distal pocket is sensitive for mutation. Interestingly, iron superoxide dismutase (FeSOD), one of the most important antioxidant enzymes, was expressed in two populations, where one displayed an acidic character (nos. 4, 5, and 13) and another was more basic (nos. 14 and 23). It should be mentioned that the acidic (major) form of FeSOD was not found in *E. coli* TG1 host cells (data not shown). These major isoforms (nos. 4, 5, and 13) completely disappeared in cells expressing P54R variant, possibly due to their distinct properties. By contrast, they could be easily detected in other samples (nos. 4, 5, 13, 14, and 23). Transformation of acidic FeSOD isoform to a more basic from was observed only upon expression of the P54R mutant. In addition, flagellin protein (no. 18) emerged in cells expressing this variant, but it was undetectable in the others. No significant difference in the overall protein expression profile was disclosed among cells expressing wild-type VHb, Y29H, and double mutant.

Discussion

Kinetics of ABTS Oxidation Catalyzed by VHb Proteins

The capability of VHb to catalyze peroxidase-like activity has recently been investigated with a variety of aromatic substrates [25, 38]. However, its reactivity is relatively low

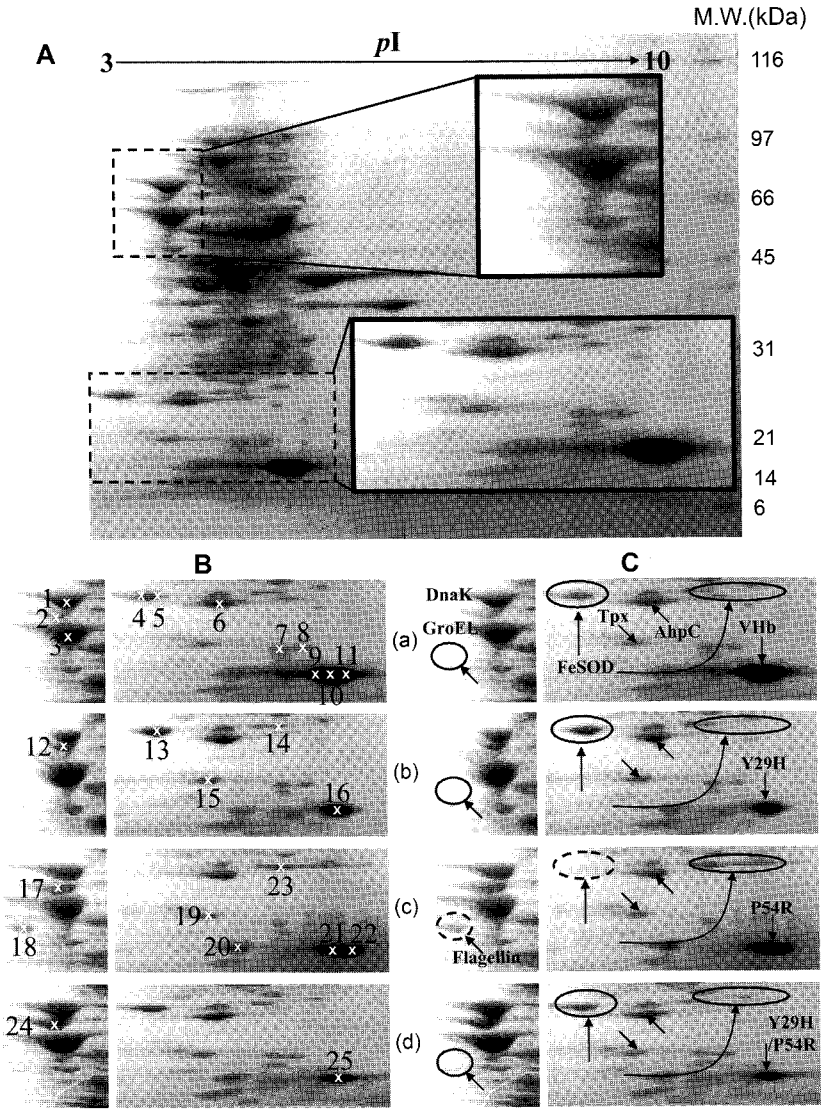

Fig. 4. Protein expression profile of *E. coli* expressing wild-type VHb electrophoresed at pH range of 3–10.
Two individual areas showing differences in protein expression were chosen for protein identification **A**. Magnified pictures of selected areas from (**B**) cells expressing wild-type VHb (a), Y29H (b), P54R (c), and Y29H/P54R (d) variants. Some protein spots were picked and identified (numbers of protein spot designated as identified protein shown in Table 2). **C**. Types of identified proteins were mapped on gels according to their corresponding spot numbers.

compared with the HRP. This may be attributable to the absence of catalytic prerequisite in its active site. Therefore, in the present study, an active site of typical peroxidase (containing catalytically conserved histidine and arginine residues) was placed into the distal pocket of VHb at positions 29 and 54, respectively (Fig. 1). Among all variants, single P54R substitution can remarkably increase k_{cat} (~15-fold compared with wild-type protein) in the reaction with the H_2O_2 molecule in the presence of aromatic substrate. This result infers that the structural rigidity provided by Pro54 hinders the catalytic moiety. Such substitution can therefore make the active site more flexible, which probably favors the peroxidase reaction [6]. Additionally, the hydrophilic nature of residues lining around the distal site has been verified to be crucial for the interaction with polar substrates like H_2O_2 in all classes of peroxidase enzyme [42]. Introduction of arginine residue may in turn increase the hydrophilicity of the distal cavity where the substrate binding and catalysis take place [34, 37]. However its K_m values for H_2O_2 and ABTS were reduced, suggesting that the introduced arginine may not be in a proper position for binding to the H_2O_2 molecule. This is surprising since results from the structure prediction demonstrated that the guanidinium group of Arg54 has been faced towards the heme cavity (Fig. 1). The distance to the iron atom of HRP appears to be ~5.7–6.0 Å [8], whereas it is only ~3.6 Å in the P54R variant. This proline residue has been replaced by alanine, and the results have

Table 2. Summary of 2-DE analysis of *E. coli* TG1 expressing wild-type VHb or its variants identified by mass spectrometry and peptide mass fingerprinting (PMF).

Spot No.	Accession No.	Description	Calculated *p*I value	Nominal mass (M_r)	Protein score[a]	Sequence coverage
1, 2, 12, 17, 24	gi|170768574	Chaperone protein DnaK	4.83	69,160	Range 82–147	Range 26–34%
3	gi|38491462	Chaperonin GroEL [*Escherichia coli*]	4.84	57,475	175	53%
4, 5, 13, 14, 23	gi|640114	*E. coli* iron superoxide dismutase (FeSOD), chain A	5.58	21,179	Range 82–89	Range 41–44%
6	gi|170172436	Alkyl hydroperoxide reductase C22 protein (AhpC)	4.92	19,250	101	54%
7	gi|15800262	Peptidyl-prolyl *cis-trans* isomerase B (rotamase B)	5.52	18,270	85	45%
8	gi|15800564	DNA starvation/stationary phase protection protein, Dps	5.72	18,684	88	50%
9, 10, 11, 16, 21, 22, 25	gi|114816	Bacterial hemoglobin (soluble cytochrome *o*)	5.31	15,821	Range 81–89	Range 41–57%
15, 19	gi|42543455	Thiol peroxidase	4.75	17,864	86, 81	47%, 36%
18	gi|89143094	Flagellin	4.50	48,885	82	32%
20	gi|15804734	Co-chaperonin GroES	5.15	10,381	83	88%

[a]Protein scores were considered to be significant ($p<0.05$) if they were greater than 80. Protein scores and sequences coverage of multiple protein spots were given as the range of values.

shown that this substitution alters the cyanide binding property [43]. Taken together, replacement of the proline residue with a charged and longer amino acid such as arginine can presumably affect the structure of the distal pocket, resulting in the alteration in binding efficiency [34]. Meanwhile, variants harboring Y29H mutations appear to decrease in catalytic performances such as catalytic constant (k_{cat}), substrate affinity (K_m), and rate of compound I formation (k_1). A plausible explanation is that the His29 is unable to bind and stabilize the bound ligand or substrate because its imidazole side chain most likely projects out of the heme group (Fig. 1). Furthermore, the distance between the distal histidine and iron center is normally 5.5–6.0 Å for peroxidases [8, 17], whereas Y29H mutation enlarges this space to approximately 10.6 Å (Fig. 1), which is inappropriate to bind H_2O_2 substrate and unable to efficiently catalyze the reaction. Moreover, Matsui *et al.* [28] have constructed myoglobin mutants with varied distal histidine and found that the formation of compound I intermediate, catalytic rate, and anion binding capability are dramatically reduced in variant harboring distal hisdine with a distance of 6.6 Å [28]. Our findings confirm such reports that the acid–base catalyst of distal histidine can be achieved only at an appropriate distance.

Absorption Spectra of VHb Variants

CO-binding spectra are basically employed to evaluate the oxidation state of hemoproteins [5, 27], since CO is able to bind only the ferrous (Fe^{2+}) protein whose Soret peak is then shifted. Because of an appropriate electronic nature of low oxidation state iron center, the synergic π^* back bonding could be formed only between CO and ferrous protein [29], not the ferric or ferrous states [27]. As demonstrated in Fig. 3, all proteins were expressed in ferric form because their Soret bands remained unchanged after the addition of dithionite. Replacement of Tyr29 with a histidine residue caused substantial spectral shift in both ferric and ferrous states to 411 nm and 424 nm, respectively, as evidenced in the Y29H and Y29H/P54R variants. Since the phenolic side chain of Tyr29 is coordinated with the heme-iron through one water molecule and plays imperative roles in ligand binding [10, 40], substitution of this position may alter the coordination architecture in the distal pocket, leading to the shift in absorption spectra. Similarly, substitution of the distal histidine with an aliphatic residue such as leucine in myoglobin has been demonstrated to shift the λ_{Soret} resulting from the loss of stabilizing residue to the heme-bound water molecule [28].

Influence of Divergent VHb Variants on Protein Profilings of *E. coli*

Although VHb protein has been shown to possess several functions in biological systems, involvement of this oxygen-binding protein in the cellular antioxidant system has not yet been reported. This study reports for the first time that expression of a high k_{cat} P54R variant significantly down-regulates FeSOD expression, as demonstrated in Fig. 4 and Table 2, whereas no other alterations in protein profile can be detected in the other variants. This inhibitory effect is independent from the expression level of VHb proteins.

FeSOD catalyzes the dismutation of superoxide anion ($O^{\cdot-}$) into O_2 and H_2O_2 and its expression is often believed to be positively regulated by the ferric uptake regulon (*fur*) [13, 16]. Fur is the major regulatory protein whose function is to control many genes involved in iron uptake as well as FeSOD and MnSOD. Fe^{2+}-Fur, the active form of this transcription factor, is able to bind the promoter region of *fur*-controlled genes and then drives the down- or upregulation of such genes. The level of iron availability directly correlates with the level of Fe^{2+}-Fur active form and induction of FeSOD expression [13, 16]. The suppressed expression of FeSOD in cells expressing the VHbH6_P54R variant is likely to be due to the reduction of intracellular level of iron atoms as a result of lower H_2O_2-induced heme degradation and iron release [31, 32, 46]. H_2O_2 can be produced by spontaneous dismutation of $O^{\cdot-}$, free radicals formed during autoxidation of hemoglobin [46]. A highly catalytic P54R variant is able to effectively eliminate reactive H_2O_2 and therefore reduces the intracellular iron level. As a consequence, the active form of ferric uptake regulatory protein (Fe^{2+}-Fur) cannot be formed, leading to the suppression of FeSOD expression. This explanation coincides with foregoing study that catalase and glutathione peroxidase are capable of protecting red blood cells from H_2O_2-induced heme degradation [30]. In the other two variants containing distal histidine, this residue plays dual roles in the autoxidation process. At acidic condition, it promotes autoxidation by facilitating an active movement of catalytic proton from solvent to the bound dioxygen *via* its imidazole side chain. This process is known as proton-catalyzed autoxidation. At the same time, it can prevent the accessible FeO_2 center from the incoming water molecule, which readily binds to heme-bound iron atom and causes autoxidation, by forming the hydrogen bond [39]. Thus, if the distal histidine residue is tilted away from the heme pocket, the rate of this reaction is more pronounced, as found in the β-chain of human hemoglobin [41]. As illustrated in Fig. 1, the side chain of His29 is positioned improperly to stabilize dioxygen in the distal cavity, and therefore, its protective effect cannot be achieved. Then, the improperly positioned distal histidine raises the radical-producing autoxidation level, leading to the increased release of iron from heme degradation. This higher iron availability ensures the expression of FeSOD *via* Fur-mediated regulation. In contrast, the optimal position of an introduced Arg54 can perhaps provide efficient stabilization of bound dioxygen through hydrogen bonding and consequently hinder the autoxidation [2]. The level of superoxide production and heme degradation is thus reduced in cells expressing this variant. This may decrease the proportion of Fur active form and thereby cause suppression of FeSOD expression (Fig. 4). Our findings open up a high feasibility of applying the P54R variant to rescue cells expressing VHb protein from the susceptibility to H_2O_2 [19]. Furthermore, this variant seems to be more applicable in large-scale fermentation, because a high rate of oxygen consumption and cellular metabolism provided by VHb probably makes cells produce more reactive oxygen species (ROS) that impede the productivity of desirable compounds. In conclusion, a highly catalytic variant of VHb (P54R) possessing ~15-fold increase in k_{cat} has successfully been constructed based on mimicking of peroxidases active sites. Replacement of Pro54 with an arginine residue contributes to the relaxed nature and higher hydrophilicity of the active site, which thereby effectively facilitates enzymatic catalysis [34, 42]. However, neither Y29H nor P54R mutation was able to promote the affinity to both peroxidase substrates. Interestingly, expression of FeSOD is suppressed in cells expressing the P54R mutant, suggesting that oxidative stress may be less produced. Potent peroxidase activity and lower autoxidation of this variant are proposed to decrease the iron availability and consequently control the Fe^{2+}-Fur level, an active transcription regulator of the FeSOD gene. H_2O_2 generated during autoxidation can be degraded rapidly by this catalytically proficient P54R variant, and it is likely that the side chain of arginine may stabilize bound dioxygen to hamper the autoxidation [2]. This superior variant of VHb can be used in a variety of applications such as a metabolic engineering tool in industrial fermentation [45, 50], a labeled enzyme in immunological assay [38], a biocatalyst in depollution of waste water [4, 9, 33], an electrochemical-redox sensor [14], and a biosensor for H_2O_2 determination [47–49].

Acknowledgments

N.T. is grateful to the Royal Golden Jubilee (RGJ) Ph.D. scholarship of Thailand Research Fund (TRF) for financial support under the supervision of V.P. This project was partially supported by an annual governmental grant under Mahidol University (2551-2555 B.E.). The authors would like to acknowledge Dr. Patcharee Panpumthong, Mr. Surasak Jiemsup, and Ms. Sirinuch Banyen for technical assistance in protein identification by mass spectrometry and peptide mass fingerprinting.

REFERENCES

1. Adams, P. A. 1990. The peroxidasic activity of the haem octapeptide microperoxidase-8(MP-8): The kinetic mechanism of the catalytic reduction of H_2O_2 by MP-8 using 2,2-azinobis-(3-ethylbenzothiazoline-6-sulphonate) (ABTS) as reducing substrate. *J. Chem. Soc. Perkin Trans.* **2:** 1407–1414.
2. Allocatelli, C. T., F. Cutruzzola, A. Brancaccio, M. Brunori, J. Qin, and G. N. La Mar. 1993. Structural and functional characterization of sperm whale myoglobin mutants: Role of arginine (E10) in ligand stabilization. *Biochemistry* **32:** 6041–6049.

3. Andersson, C. I., C. Arfvidsson, P. T. Kallio, K. G. Wahlund, and L. Bulow. 2003. Enhanced ribosome and tRNA contents in *Escherichia coli* expressing a truncated *Vitreoscilla* hemoglobin mutant analyzed by flow field-flow fractionation. *Biotechnol. Lett.* **25:** 1499–1504.
4. Arseguel, D. and M. Baboulne. 2004. Removal of phenol from coupling of talc and peroxidase: Application for depollution of waste water containing phenolic compounds. *J. Chem. Technol. Biotechnol.* **61:** 331–335.
5. Ascenzi, P., M. Brunori, M. Coletta, and A. Desideri. 1989. pH effects on the haem iron co-ordination state in the nitric oxide and deoxy derivatives of ferrous horseradish peroxidase and cytochrome *c* peroxidase. *Biochem. J.* **258:** 473–478.
6. Bauer, F. and H. Sticht. 2007. A proline to glycine mutation in the Lck SH3-domain affects conformational sampling and increases ligand binding affinity. *FEBS Lett.* **581:** 1555–1560.
7. Beale, S. I. 1990. Biosynthesis of the tetrapyrrole pigment precursor, delta-aminolevulinic acid, from glutamate. *Plant Physiol.* **93:** 1273–1279.
8. Berglund, G. I., G. H. Carlsson, A. T. Smith, H. Szoke, A. Henriksen, and J. Hajdu. 2002. The catalytic pathway of horseradish peroxidase at high resolution. *Nature* **417:** 463–468.
9. Bodalo, A., J. L. Gomez, E. Gomez, A. M. Hidalgo, M. Gomez, and A. M. Yelo. 2007. Elimination of 4-chlorophenol by soybean peroxidase and hydrogen peroxide: Kinetic model and intrinsic parameters. *Biochem. Eng. J.* **34:** 242–247.
10. Bolognesi, M., A. Boffi, M. Coletta, A. Mozzarelli, A. Pesce, C. Tarricone, and P. Ascenzi. 1999. Anticooperative ligand binding properties of recombinant ferric *Vitreoscilla* homodimeric hemoglobin: A thermodynamic, kinetic and X-ray crystallographic study. *J. Mol. Biol.* **291:** 637–650.
11. Bradford, M. M. 1976. A rapid and sensitive method for the quantitation of microgram quantities of protein utilizing the principle of protein-dye binding. *Anal. Biochem.* **72:** 248–254.
12. Delano, W. L. 1998. The PyMOL Molecular Graphic System. Delano Scientific LLC, San Carlos, CA (http://www.pymol.org).
13. Dubrac, S. and D. Touati. 2002. Fur-mediated transcriptional and post-transcriptional regulation of FeSOD expression in *Escherichia coli*. *Microbiology* **148:** 147–156.
14. Fan, C., J. Zhong, R. Guan, and G. Li. 2003. Direct electrochemical characterization of *Vitreoscilla* sp. hemoglobin entrapped in organic films. *Biochim. Biophys. Acta* **1649:** 123–126.
15. Farres, J. and P. T. Kallio. 2002. Improved cell growth in tobacco suspension cultures expressing *Vitreoscilla* hemoglobin. *Biotechnol. Prog.* **18:** 229–233.
16. Fee, J. A. 1991. Regulation of *sod* genes in *Escherichia coli*: Relevance to superoxide dismutase function. *Mol. Microbiol.* **5:** 2599–2610.
17. Finzel, B. C., T. L. Poulos, and J. Kraut. 1984. Crystal structure of yeast cytochrome *c* peroxidase refined at 1.7-A resolution. *J. Biol. Chem.* **259:** 13027–13036.
18. Frey, A. D., B. T. Oberle, J. Farres, and P. T. Kallio. 2004. Expression of *Vitreoscilla* haemoglobin in tobacco cell cultures relieves nitrosative stress *in vivo* and protects from NO *in vitro*. *Plant Biotechnol. J.* **2:** 221–231.
19. Geckil, H., S. Gencer, H. Kahraman, and S. O. Erenler. 2003. Genetic engineering of *Enterobacter aerogenes* with the *Vitreoscilla* hemoglobin gene: Cell growth, survival, and antioxidant enzyme status under oxidative stress. *Res. Microbiol.* **154:** 425–431.
20. George, P. 1953. The chemical nature of the second hydrogen peroxide compound formed by cytochrome *c* peroxidase and horseradish peroxidase. I. Titration with reducing agents. *Biochem. J.* **54:** 267–276.
21. Isarankura-Na-Ayudhya, C., P. Panpumthong, T. Tangkosakul, S. Boonpangrak, and V. Prachayasittikul. 2008. Shedding light on the role of *Vitreoscilla* hemoglobin on cellular catabolic regulation by proteomic analysis. *Int. J. Biol. Sci.* **4:** 71–80.
22. Kaur, R., R. Pathania, V. Sharma, S. C. Mande, and K. L. Dikshit. 2002. Chimeric *Vitreoscilla* hemoglobin (VHb) carrying a flavoreductase domain relieves nitrosative stress in *Escherichia coli*: New insight into the functional role of VHb. *Appl. Environ. Microbiol.* **68:** 152–160.
23. Khosla, C. and J. E. Bailey. 1988. Heterologous expression of a bacterial haemoglobin improves the growth properties of recombinant *Escherichia coli*. *Nature* **331:** 633–635.
24. Khosla, C., J. E. Curtis, J. DeModena, U. Rinas, and J. E. Bailey. 1990. Expression of intracellular hemoglobin improves protein synthesis in oxygen-limited *Escherichia coli*. *Biotechnology (NY)* **8:** 849–853.
25. Kvist, M., E. S. Ryabova, E. Nordlander, and L. Bulow. 2007. An investigation of the peroxidase activity of *Vitreoscilla* hemoglobin. *J. Biol. Inorg. Chem.* **12:** 324–334.
26. Ling, K. Q. and L. M. Sayre. 2005. Horseradish peroxidase-mediated aerobic and anaerobic oxidations of 3-alkylindoles. *Bioorg. Med. Chem.* **13:** 3543–3551.
27. Liu, C. Y. and D. A. Webster. 1974. Spectral characteristics and interconversions of the reduced oxidized and oxygenated forms of purified cytochrome *o*. *J. Biol. Chem.* **249:** 4261–4266.
28. Matsui, T., S. Ozaki, E. Liong, G. N. Phillips Jr., and Y. Watanabe. 1999. Effects of the location of distal histidine in the reaction of myoglobin with hydrogen peroxide. *J. Biol. Chem.* **274:** 2838–2844.
29. Miessler, G. L. and D. A. Tarr. 2004. *Inorganic Chemistry*, 3rd Ed. Prentice Hall, Upper Saddle River, New Jersey.
30. Nagababu, E., F. J. Chrest, and J. M. Rifkind. 2003. Hydrogen-peroxide-induced heme degradation in red blood cells: The protective roles of catalase and glutathione peroxidase. *Biochim. Biophys. Acta* **1620:** 211–217.
31. Nagababu, E. and J. M. Rifkind. 2000. Heme degradation during autoxidation of oxyhemoglobin. *Biochem. Biophys. Res. Commun.* **273:** 839–845.
32. Nagababu, E. and J. M. Rifkind. 2000. Reaction of hydrogen peroxide with ferrylhemoglobin: Superoxide production and heme degradation. *Biochemistry* **39:** 12503–12511.
33. Patapas, J., M. M. Al-Ansari, K. E. Taylor, J. K. Bewtra, and N. Biswas. 2007. Removal of dinitrotoluenes from water *via* reduction with iron and peroxidase-catalyzed oxidative polymerization: A comparison between *Arthromyces ramosus* peroxidase and soybean peroxidase. *Chemosphere* **67:** 1485–1491.
34. Redaelli, C., E. Monzani, L. Santagostini, L. Casella, A. M. Sanangelantoni, R. Pierattelli, and L. Banci. 2002. Characterization and peroxidase activity of a myoglobin mutant containing a distal arginine. *Chembiochem* **3:** 226–233.
35. Rodriguez-Lopez, J. N., A. T. Smith, and R. N. Thorneley. 1996. Role of arginine 38 in horseradish peroxidase. A critical

residue for substrate binding and catalysis. *J. Biol. Chem.* **271:** 4023–4030.

36. Roos, V., C. I. Andersson, C. Arfvidsson, K. G. Wahlund, and L. Bulow. 2002. Expression of double *Vitreoscilla* hemoglobin enhances growth and alters ribosome and tRNA levels in *Escherichia coli*. *Biotechnol. Prog.* **18:** 652–656.
37. Schiodt, C. B., N. C. Veitch, and K. G. Welinder. 2007. Roles of distal arginine in activity and stability of *Coprinus cinereus* peroxidase elucidated by kinetic and NMR analysis of the Arg51Gln, -Asn, -Leu, and -Lys mutants. *J. Inorg. Biochem.* **101:** 336–347.
38. Suwanwong, Y., M. Kvist, C. Isarankura-Na-Ayudhya, N. Tansila, L. Bulow, and V. Prachayasittikul. 2006. Chimeric antibody-binding *Vitreoscilla* hemoglobin (VHb) mediates redox-catalysis reaction: New insight into the functional role of VHb. *Int. J. Biol. Sci.* **2:** 208–215.
39. Suzuki, T., Y. H. Watanabe, M. Nagasawa, A. Matsuoka, and K. Shikama. 2000. Dual nature of the distal histidine residue in the autoxidation reaction of myoglobin and hemoglobin comparison of the H64 mutants. *Eur. J. Biochem.* **267:** 6166–6174.
40. Tarricone, C., A. Galizzi, A. Coda, P. Ascenzi, and M. Bolognesi. 1997. Unusual structure of the oxygen-binding site in the dimeric bacterial hemoglobin from *Vitreoscilla* sp. *Structure* **5:** 497–507.
41. Tsuruga, M., A. Matsuoka, A. Hachimori, Y. Sugawara, and K. Shikama. 1998. The molecular mechanism of autoxidation for human oxyhemoglobin. Tilting of the distal histidine causes nonequivalent oxidation in the beta chain. *J. Biol. Chem.* **273:** 8607–8615.
42. Veitch, N. C. 2004. Horseradish peroxidase: A modern view of a classic enzyme. *Phytochemistry* **65:** 249–259.
43. Verma, S., S. Patel, R. Kaur, Y. T. Chung, B. T. Duk, K. L. Dikshit, B. C. Stark, and D. A. Webster. 2005. Mutational study of the bacterial hemoglobin distal heme pocket. *Biochem. Biophys. Res. Commun.* **326:** 290–297.
44. Wakabayashi, S., H. Matsubara, and D. A. Webster. 1986. Primary sequence of a dimeric bacterial haemoglobin from *Vitreoscilla*. *Nature* **322:** 481–483.
45. Wei, X. X. and G. Q. Chen. 2008. Applications of the VHb gene *vgb* for improved microbial fermentation processes. *Methods Enzymol.* **436:** 273–287.
46. Winterbourn, C. C. 1985. Free-radical production and oxidative reactions of hemoglobin. *Environ. Health Perspect.* **64:** 321–330.
47. Yang, G., R. Yuan, and Y. Q. Chai. 2008. A high-sensitive amperometric hydrogen peroxide biosensor based on the immobilization of hemoglobin on gold colloid/L-cysteine/gold colloid/nanoparticles Pt-chitosan composite film-modified platinum disk electrode. *Colloids Surf. B Biointerfaces* **61:** 93–100.
48. Zhang, J. and M. Oyama. 2004. A hydrogen peroxide sensor based on the peroxidase activity of hemoglobin immobilized on gold nanoparticles-modified ITO electrode. *Electrochim. Acta* **50:** 85–90.
49. Zhang, K., L. Mao, and R. Cai. 2000. Stopped-flow spectrophotometric determination of hydrogen peroxide with hemoglobin as catalyst. *Talanta* **51:** 179–186.
50. Zhang, L., Y. Li, Z. Wang, Y. Xia, W. Chen, and K. Tang. 2007. Recent developments and future prospects of *Vitreoscilla* hemoglobin application in metabolic engineering. *Biotechnol. Adv.* **25:** 123–136.